COMMUNICATION

Check for updates

Mössbauer and mass spectrometry support for iron(II) catalysts in enantioselective C–H activation†

Joachim Loup, [ID] [a] Tobias Parchomyk,[a] Stefan Lülf,[a] Serhiy Demeshko,[b] Franc Meyer, [ID] [b] Konrad Koszinowski [ID] *[a] and Lutz Ackermann [ID] *[a]

A combination of electrospray-ionization mass spectrometry and Mössbauer spectroscopy was used to investigate the species generated *in situ* in highly enantioselective Fe/NHC-catalyzed C–H alkylations. The findings indicate an organometallic iron(II)–NHC species to be of key relevance in the asymmetric catalysis.

Iron has emerged as a sustainable, inexpensive and non-toxic alternative to noble transition metals for catalysis,[1] and applications to cross-coupling chemistry[2] and C–H activation[3] have experienced a considerable development in recent years. Notably, the association of N-heterocyclic carbene (NHC) ligands with iron is of particular interest and has been exploited for C–C and C–X forming processes.[4]
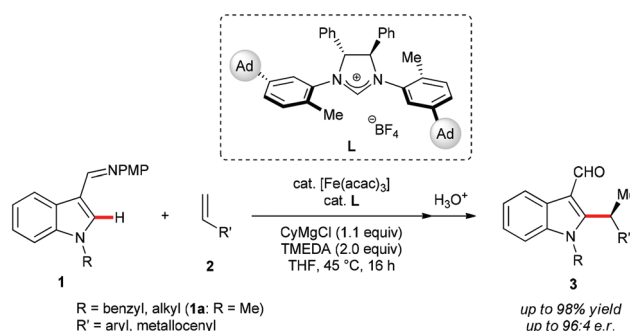
Within our program on iron-catalyzed C–H activation,[5] we have very recently developed the first example of enantioselective iron-catalyzed C–H functionalizations by inner-sphere organometallic C–H activation.[6] Key to success was the design of the novel NHC ligand **L** featuring remote *meta*-adamantyl substituents (Scheme 1). While detailed kinetic studies and deuterium labelling experiments were performed to delineate the *modus operandi* of the transformation, the oxidation state and coordination sphere of the active catalyst remained thus far elusive.

Indeed, in iron/NHC catalyzed C–H activations,[6,7] as well as in related low-valent cobalt/NHC-catalyzed C–H activations,[8] the active catalyst is generated *in situ* from a metal salt and a imidazol(in)ium NHC precursor in the presence of a Grignard reagent. The organometallic reagent is assumed to play a dual role serving both as base and reductant, but no well-defined complex has been so far isolated or characterized in this

context, with the notable exception of Tatsumi/Ohki employing a half sandwich Fe(II)/NHC complex for undirected C–H borylations.[9]

Based on preliminary mechanistic studies and previous reports,[10] we initially proposed an organometallic Fe/NHC species to be the active catalyst and the key C–H cleavage event to occur *via* a ligand-to-ligand hydrogen-transfer (LLHT) manifold.[11] On the contrary, Yoshikai originally proposed a low-valent Fe/NHC complex with an oxidation state <+2 generated through the reduction of the iron(III) pre-catalyst by the Grignard reagent to be operative in a racemic hydroarylation of vinylarenes and alkynes with indoles, and the C–H activation step to occur *via* C–H oxidative addition.[7] It is noteworthy that Yoshikai attributed the requirement of an excess of the Grignard reagent to the possible formation of ferrate species.

In the course of our earlier studies, we observed that Fe(acac)₃ and FeCl₂ pre-catalysts, despite their different oxidation states and counterions, gave comparable conversions and enantio-selectivities. This observation was suggestive of the iron precursors being transformed by the Grignard reagent to the same catalytically competent iron species. Another possibility is the *in situ* formation of organoferrates, in agreement with recent reports that the nature of the iron precursor has very little effect on the transmetallation reactions with

[a]*Institut für Organische und Biomolekulare Chemie, Universität Göttingen, Tammannstraße 2, 37077 Göttingen, Germany.*
E-mail: Konrad.Koszinowski@chemie.uni-goettingen.de,
Lutz.Ackermann@chemie.uni-goettingen.de
[b]*Institut für Anorganische Chemie, Universität Göttingen, Tammannstraße 4, 37077 Göttingen, Germany.*
†Electronic supplementary information (ESI) available: Experimental procedures, additional spectra. See DOI: 10.1039/c9dt00705a

Scheme 1 Asymmetric iron-catalyzed C–H alkylation.

organometallic species to form such complexes.[12] These observations raised the question as to the nature of the active catalyst and its mode of action, and highlight the need for detailed, comprehensive mechanistic studies to unravel fundamental aspects of iron-catalyzed C–H activations. Such mechanistic insights have recently been gained for iron-catalyzed Kumada–Corriu-type cross-coupling reactions *via* Mössbauer spectroscopy and mass spectrometry.[12,13] These reports highlighted the dynamic nature and remarkable complexity of organometallic iron chemistry.

Hence, we became interested in the application of electrospray-ionization (ESI) mass spectrometry and Mössbauer spectroscopy to elucidate the key intermediates formed *in situ* in the enantioselective iron-catalyzed C–H alkylation. Mössbauer spectroscopy has the advantage of probing the entire population of iron species, regardless of their individual charge. We decided to follow a step-by-step approach and therefore initiated our investigation by probing the species formed in the reaction between the iron pre-catalyst, the Grignard reagent and N,N,N',N'-tetramethylethane-1,2-diamine (TMEDA) in THF, without the NHC precursor or the indole substrate. Negative-ion mode ESI mass spectra of a solution of $Fe(acac)_3$ treated with 8.0 equiv. of CyMgCl in the presence of TMEDA (4.0 equiv.) showed a mixture of various organoferrate species, among which $Cy_3Fe(II)^-$ and $Cy_4Fe(III)^-$ predominated (Fig. 1a). Previous work had already established the formation of abundant organoferrate anions upon transmetallation of iron precursors with Grignard reagents.[12] Although ESI mass spectrometry cannot directly detect any neutral species, the observation of small amounts of the anions $Cy_5Fe_2^-$ and $Cy_4Fe_2Cl^-$ – both with iron in an average oxidation state of II – indicated the presence of neutral organoiron complexes, such as Cy_2Fe or CyFeCl, which supposedly reacted with $Cy_3Fe(II)^-$ to afford the dinuclear aggregates. The low abundance of the dinuclear anions can be ascribed to the addition of TMEDA, which had previously been shown to prevent the formation of polynuclear organoferrates.[10a,12,14] All of the detected organoferrates were found to be highly unstable, presumably due to β-hydride elimination, and completely disappeared within minutes. Experiments conducted with the more stable and user-friendly PhMgCl were hence performed as well. PhMgCl had previously been shown to effect the desired C–H alkylation as well, albeit with a slightly diminished performance.[6] Likewise, iron(II) and iron(III) phenylferrates were observed by ESI-MS in the reaction of $Fe(acac)_3$ with PhMgCl in the presence of TMEDA (Fig. S1†), being in full agreement with previous findings.[10a,12,15]

We next analyzed a frozen solution of $^{57}FeCl_2/CyMgCl/$TMEDA by ^{57}Fe Mössbauer spectroscopy at 80 K (Fig. 1b). The obtained spectrum featured the signatures of two iron species, which were assigned to a major high-spin iron(III) species and a minor low-coordinate iron(II) species, in line with the formation of $Cy_4Fe(III)^-$ and $Cy_3Fe(II)^-$ observed by ESI-MS. The remarkable formation of a dominating iron(III) species from the iron(II) precursor in the presence of Grignard reagents and the absence of any external oxidant is attributed to disproportionation with concomitant formation of a low-valent iron
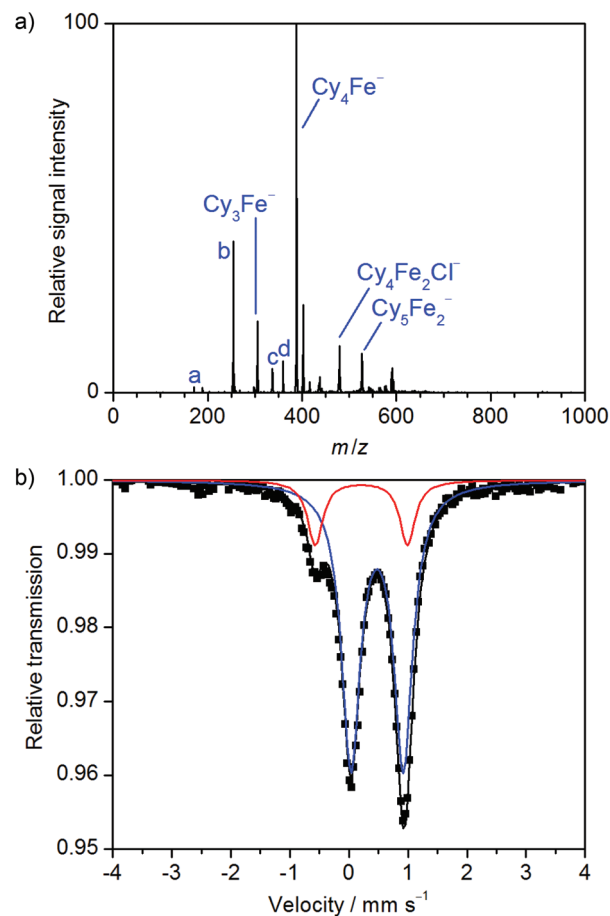
Fig. 1 (a) Negative-ion mode ESI mass spectrum of a solution of the products formed in the reaction of $Fe(acac)_3$ (10 mM) with TMEDA (4.0 equiv.) and CyMgCl (8.0 equiv.) in THF; $a = [Cy,Fe,O_2]^-$, $b = [Cy_2,Fe,O_2]^-$, $c = [Cy_3,Fe,O_2]^-$, $d = Cy_4Al^-$. Ions a–c resulted from reactions with residual traces of oxygen, d from an aluminum contamination. (b) Mössbauer spectrum of a frozen solution ($T = 80$ K) of the products formed in the reaction of $^{57}FeCl_2$ (5.0 mM), TMEDA (4.0 equiv.) and CyMgCl (8.0 equiv.) in THF; components of the fit: δ(blue) = 0.48 mm s^{-1}, ΔE_Q(blue) = 0.89 mm s^{-1}, rel. int. = 84%; δ(red) = 0.21 mm s^{-1}, ΔE_Q(red) = 1.56 mm s^{-1}, rel. int. = 16%.

species.[12,16] Interestingly, we did not detect any $Cy_4Fe(IV)$, which had been observed in a related setting.[19] The instability of the cyclohexylferrates was further highlighted by ^{57}Fe Mössbauer spectroscopic analysis of the same reaction after it was allowed to warm to 23 °C (Fig. S3†). The spectrum showed the complete disappearance of the iron(II) ate complex, a reduced amount of $Cy_4Fe(III)^-$ and the emergence of a new dominant species, whose unspecific doublet unfortunately does not allow for assignment.

A similar spectrum was obtained from the reaction of $^{57}FeCl_2$ with PhMgCl in the presence of TMEDA (Fig. S4†), indicating the formation of the phenylferrates $Ph_3Fe(II)^-$ and $Ph_4Fe(III)^-$, being in line with the ESI-MS results and previous reports.[10a,12] The parameters of the Mössbauer doublet assigned to $Ph_3Fe(II)^-$ (δ = 0.20 mm s^{-1}, ΔE_Q(red) = 1.44 mm s^{-1}) are indeed very similar to those reported for the

closely related $Mes_3Fe(II)^-$ (δ = 0.21 mm s^{-1}, ΔE_Q = 1.43 mm s^{-1}).[13h] The dimeric dianion $[\{Ph_2Fe(\mu\text{-}Ph)\}_2]^{2-}$ (δ = 0.34 mm s^{-1} and ΔE_Q = 2.28 mm s^{-1} at 80 K), previously obtained from the low temperature reaction of $Fe(acac)_3$ and PhMgBr in THF, has a higher isomer shift and much larger quadrupole splitting, and the more reduced neutral tetramer $Fe_4(\mu\text{-}Ph)_6(solv)_x$ (δ = 0.60 mm s^{-1} and ΔE_Q = 0.84 mm s^{-1} at 80 K) has a significantly higher isomer shift.[13j] As the catalyzed C–H activation was found to be completely shut down in the absence of the ligand,[6] the observed ligand-free organoferrates are assumed to be catalytically inactive.
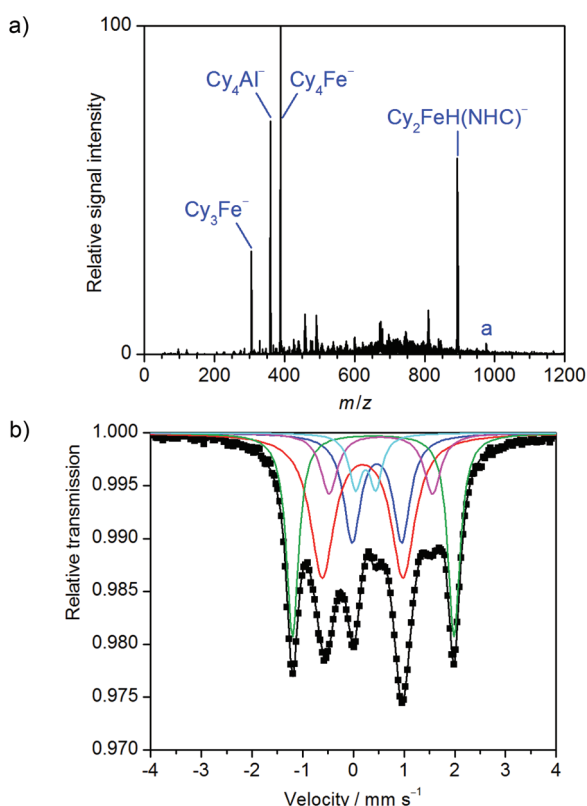
Subsequently, similar experiments were performed in the presence of the chiral NHC precursor **L** (Fig. 2a). While the homoleptic ferrates remained present in the solution, two newly formed iron(II) species could also be observed, namely $Cy_3Fe(NHC)^-$ and $Cy_2FeH(NHC)^-$ (Fig. S5 and S6†). The latter, with a significantly higher intensity, is believed to result from β-hydrogen elimination of the former. Interestingly, no NHC

Fig. 2 (a) Negative-ion mode ESI mass spectrum of a solution of the products formed in the reaction of $Fe(acac)_3$ (10 mM) with TMEDA (4.0 equiv.), CyMgCl (8.0 equiv.) and **L** (1.0 equiv.) in THF; a = $[Fe(NHC)Cy_3]^-$. NHC = $C_{49}H_{54}N_2$. Cy_4Al^- resulted from an aluminum contamination. (b) Mössbauer spectrum of a frozen solution (T = 80 K) of the products formed in the reaction of $^{57}FeCl_2$ (5.0 mM), TMEDA (4.0 equiv.), **L** (1.0 equiv.) and CyMgCl (8.0 equiv.) in THF; components of the fit: δ(red) = 0.18 mm s^{-1}, ΔE_Q(red) = 1.59 mm s^{-1}, rel. int. = 36%; δ(green) = 0.39 mm s^{-1}, ΔE_Q(green) = 3.19 mm s^{-1}, rel. int. = 27%; δ(blue) = 0.46 mm s^{-1}, ΔE_Q(blue) = 0.98 mm s^{-1}, rel. int. = 19%; δ(magenta) = 0.54 mm s^{-1}, ΔE_Q(magenta) = 2.04 mm s^{-1}, rel. int. = 11%; δ(cyan) = 0.24 mm s^{-1}, ΔE_Q(cyan) = 0.40 mm s^{-1}, rel. int. = 7%.

complexes of iron(III) or low-valent iron were detected, suggesting the selective formation of Fe(II)/NHC species in the reaction.

When a similar experiment was performed using PhMgCl, no Fe/NHC species could be observed (Fig. S7†). Yet, the relative intensity of the iron(II) ate complex was noticeably reduced, which presumably indicates its consumption to form neutral species not detectable by ESI mass spectrometry. Besides, no magnesium-NHC complexes or residual imidazolinium salt could be observed by positive-mode ESI-MS in any of the experiments (Fig. S8†), providing evidence for the NHC to coordinate to the iron catalyst, and not to Mg(II).

When a frozen solution of $^{57}FeCl_2$/**L**/CyMgCl/TMEDA was analyzed by Mössbauer spectroscopy, a rather complicated spectrum could be observed which has been simulated well assuming five subspectra.[20] Two subspectra (Fig. 2b, blue and red) are almost identical to the previously observed ferrates (Fig. 1b). The most intense new signal (Fig. 2b, green, 27% intensity) with a large quadrupole splitting of 3.19 mm s^{-1} but with quite a low isomer shift of 0.39 mm s^{-1} can be assigned to a low-coordinate iron(II) high-spin complex, most likely trigonal-planar $Cy_2Fe(NHC)$,[21] in line with ESI mass spectrometry (see above). It should be noted that the isomer shifts of $L_2Fe(NHC)$ complexes can vary depending on the covalency of the Fe–C bond. Examples include δ = 0.33 to 0.35 mm s^{-1} at 80 K for $[(Me_3Si)CH_2]_2Fe(NHC)$,[21c] δ = 0.33 mm s^{-1} at 200 K for $(Ph_2C=CPh)_2Fe(NHC)$,[21d] or δ = 0.44 to 0.57 mm s^{-1} at 5 K for $(1,3\text{-dioxan-2-ylethyl})_2Fe(NHC)$;[21a] all these complexes were shown to adopt a high-spin Fe(II) state. Another newly formed species (magenta), with a higher isomer shift of 0.54 mm s^{-1} together with a lower quadrupole splitting of 2.04 mm s^{-1}, may indicate a more symmetric iron(II) high-spin species with a higher coordination number such as $Cy_3Fe(NHC)^-$, as observed by ESI-MS (see Fig. S5†). An additional minor species (Fig. 2b, cyan) was also observed in the ^{57}Fe Mössbauer spectrum of the reaction with CyMgCl, but its non-characteristic doublet does not allow for further assignment. Two similar iron(II) species were also detected in the analogous reaction with PhMgCl (Fig. S9†). No species related to the minor uncharacteristic signal observed previously was however detected in this system. It is hence believed that this species was formed *via* β-hydride elimination from the $Cy_2Fe(NHC)$ complex. This hypothesis is substantiated by the observation that, when the sample was prepared at higher temperatures, this species (cyan) became more pronounced, while the intensity of the $Cy_2Fe(NHC)$ signal (green) was reduced (Fig. S10†).

Thereafter, additional experiments in the presence of the indole substrate **1a** were conducted. Besides the previously observed species, $[Cy_4Fe(indole)]^-$ was observed by ESI-MS analysis of the reaction of $^{57}FeCl_2$/CyMgCl/TMEDA/**L**/**1a** (Fig. S11†). Yet, this species is believed to be catalytically irrelevant in the C–H activation due to the absence of the NHC ligand. ESI-MS analysis of the reaction of $^{57}FeCl_2$/PhMgCl/TMEDA/**L**/**1a** showed no new species, but the almost complete disappearance of the $Ph_3Fe(II)^-$ ferrate (Fig. S12†). Its consumption is suggestive of a reaction between the iron(II) ate complex, or a species in equili-

brium with it, and the substrate **1a** to form a neutral species. Therefore, this observation is suggestive of an iron(II) species to be involved as intermediate in the C–H activation.

No new species or significant changes upon the addition of substrate **1a** were observed by [57]Fe Mössbauer spectroscopy analysis of the analogous reactions with either CyMgCl or PhMgCl, except a slight reduction of the species believed to be R_2Fe(NHC) (Fig. S13 and S14†).

In summary, we report on the unprecedented application of ESI-MS and [57]Fe Mössbauer spectroscopy to study the mechanism of iron-catalyzed asymmetric C–H activations. Our experimental findings provide support for the formation of an organometallic Fe(II)/NHC complex as an intermediate in the iron-catalyzed enantioselective C–H alkylation of indoles. Furthermore, no interaction between iron and TMEDA was observed in any of the experiments, which suggests that TMEDA coordinates the Mg(II) ions and does not interact with the iron catalyst.

Conflicts of interest

There are no conflicts to declare.

Acknowledgements

References

1 (a) A. Fürstner, *ACS Cent. Sci.*, 2016, **2**, 778; (b) I. Bauer and H.-J. Knölker, *Chem. Rev.*, 2015, **115**, 3170; (c) C. Bolm, J. Legros, J. Le Paih and L. Zani, *Chem. Rev.*, 2004, **104**, 6217.

2 (a) A. Piontek, E. Bisz and M. Szostak, *Angew. Chem., Int. Ed.*, 2018, **57**, 11116; (b) T. L. Mako and J. A. Byers, *Inorg. Chem. Front.*, 2016, **3**, 766; (c) C. Cassani, G. Bergonzini and C.-J. Wallentin, *ACS Catal.*, 2016, **6**, 1640; (d) E. Nakamura, T. Hatakeyama, S. Ito, K. Ishizuka, L. Ilies and M. Nakamura, *Org. React.*, 2014, **83**, 1; (e) R. Jana, T. P. Pathak and M. S. Sigman, *Chem. Rev.*, 2011, **111**, 1417; (f) E. Nakamura and N. Yoshikai, *J. Org. Chem.*, 2010, **75**, 6061; (g) W. M. Czaplik, M. Mayer, J. Cvengroš and A. J. von Wangelin, *ChemSusChem*, 2009, **2**, 396; (h) B. D. Sherry and A. Fürstner, *Acc. Chem. Res.*, 2008, **41**, 1500.

3 (a) N. Yoshikai, *Isr. J. Chem.*, 2017, **57**, 1117; (b) R. Shang, L. Ilies and E. Nakamura, *Chem. Rev.*, 2017, **117**, 9086; (c) G. Cera and L. Ackermann, *Top. Curr. Chem.*, 2016, **374**, 57.

4 (a) C. Johnson and M. Albrecht, *Coord. Chem. Rev.*, 2017, **352**, 1; (b) K. Riener, S. Haslinger, A. Raba, M. P. Högerl, M. Cokoja, W. A. Herrmann and F. E. Kühn, *Chem. Rev.*,

2014, **114**, 5215; (c) D. Bézier, J.-B. Sortais and C. Darcel, *Adv. Synth. Catal.*, 2013, **355**, 19.

5 Selected examples: (a) J. Mo, T. Müller, J. C. A. Oliveira and L. Ackermann, *Angew. Chem., Int. Ed.*, 2018, **57**, 7719; (b) Z. Shen, G. Cera, T. Haven and L. Ackermann, *Org. Lett.*, 2017, **19**, 3795; (c) G. Cera, T. Haven and L. Ackermann, *Chem. Commun.*, 2017, **53**, 6460; (d) G. Cera, T. Haven and L. Ackermann, *Chem. – Eur. J.*, 2017, **23**, 3577; (e) G. Cera, T. Haven and L. Ackermann, *Angew. Chem., Int. Ed.*, 2016, **55**, 1484; (f) K. Graczyk, T. Haven and L. Ackermann, *Chem. – Eur. J.*, 2015, **21**, 8812; (g) Q. Gu, H. H. Al Mamari, K. Graczyk, E. Diers and L. Ackermann, *Angew. Chem., Int. Ed.*, 2014, **53**, 3868.

6 J. Loup, D. Zell, J. C. A. Oliveira, H. Keil, D. Stalke and L. Ackermann, *Angew. Chem., Int. Ed.*, 2017, **56**, 14197.

7 M. Y. Wong, T. Yamakawa and N. Yoshikai, *Org. Lett.*, 2015, **17**, 442.

8 (a) N. Sauermann, J. Loup, D. Kootz, V. R. Yatham, A. Berkessel and L. Ackermann, *Synthesis*, 2017, **49**, 3476; (b) M. Moselage, N. Sauermann, S. C. Richter and L. Ackermann, *Angew. Chem., Int. Ed.*, 2015, **54**, 6352; (c) J. Li and L. Ackermann, *Chem. – Eur. J.*, 2015, **21**, 5718; (d) B. Punji, W. Song, G. A. Shevchenko and L. Ackermann, *Chem. – Eur. J.*, 2013, **19**, 10605; (e) K. Gao and N. Yoshikai, *J. Am. Chem. Soc.*, 2013, **135**, 9279; (f) Z. Ding and N. Yoshikai, *Angew. Chem., Int. Ed.*, 2013, **52**, 8574; (g) W. Song and L. Ackermann, *Angew. Chem., Int. Ed.*, 2012, **51**, 8251; (h) K. Gao and N. Yoshikai, *Chem. Commun.*, 2012, **48**, 4305. Selected reviews: (i) M. Moselage, J. Li and L. Ackermann, *ACS Catal.*, 2016, **6**, 498; (j) K. Gao and N. Yoshikai, *Acc. Chem. Res.*, 2014, **47**, 1208; (k) L. Ackermann, *J. Org. Chem.*, 2014, **79**, 8948.

9 (a) T. Hatanaka, Y. Ohki and K. Tatsumi, *Chem. – Asian J.*, 2010, **5**, 1657; (b) Y. Ohki, T. Hatanaka and K. Tatsumi, *J. Am. Chem. Soc.*, 2008, **130**, 17174.

10 (a) T. Parchomyk and K. Koszinowski, *Chem. – Eur. J.*, 2016, **22**, 15609; (b) R. B. Bedford, P. B. Brenner, D. Elorriaga, J. N. Harvey and J. Nunn, *Dalton Trans.*, 2016, **45**, 15811; (c) R. B. Bedford, P. B. Brenner, E. Carter, P. M. Cogswell, M. F. Haddow, J. N. Harvey, D. M. Murphy, J. Nunn and C. H. Woodall, *Angew. Chem., Int. Ed.*, 2014, **53**, 1804; (d) M. D. Greenhalgh and S. P. Thomas, *J. Am. Chem. Soc.*, 2012, **134**, 11900; (e) E. Shirakawa, D. Ikeda, S. Masui, M. Yoshida and T. Hayashi, *J. Am. Chem. Soc.*, 2012, **134**, 272.

11 (a) D. Zell, M. Bursch, V. Müller, S. Grimme and L. Ackermann, *Angew. Chem., Int. Ed.*, 2017, **56**, 10378; (b) O. Eisenstein, J. Milani and R. N. Perutz, *Chem. Rev.*, 2017, **117**, 8710; (c) J. Guihaumé, S. Halbert, O. Eisenstein and R. N. Perutz, *Organometallics*, 2012, **31**, 1300; (d) L. Ackermann, *Chem. Rev.*, 2011, **111**, 1315.

12 T. Parchomyk, S. Demeshko, F. Meyer and K. Koszinowski, *J. Am. Chem. Soc.*, 2018, **140**, 9709.

13 (a) J. D. Sears, P. G. N. Neate and M. L. Neidig, *J. Am. Chem. Soc.*, 2018, **140**, 11872; (b) T. Parchomyk and K. Koszinowski, *Synthesis*, 2017, **49**, 3269; (c) R. B. Bedford,

Acc. Chem. Res., 2015, **48**, 1485; (*d*) S. H. Carpenter and M. L. Neidig, *Isr. J. Chem.*, 2017, **57**, 1106; (*e*) S. B. Muñoz III, S. L. Daifuku, J. D. Sears, T. M. Baker, S. H. Carpenter, W. W. Brennessel and M. L. Neidig, *Angew. Chem., Int. Ed.*, 2018, **57**, 6496; (*f*) J. L. Kneebone, W. W. Brennessel and M. L. Neidig, *J. Am. Chem. Soc.*, 2017, **139**, 6988; (*g*) S. B. Muñoz III, S. L. Daifuku, W. W. Brennessel and M. L. Neidig, *J. Am. Chem. Soc.*, 2016, **138**, 7492; (*h*) S. L. Daifuku, M. H. Al-Afyouni, B. E. R. Snyder, J. L. Kneebone and M. L. Neidig, *J. Am. Chem. Soc.*, 2014, **136**, 9132; (*i*) M. H. Al-Afyouni, K. L. Fillman, W. W. Brennessel and M. L. Neidig, *J. Am. Chem. Soc.*, 2014, **136**, 15457–15460; (*j*) S. H. Carpenter, T. M. Baker, S. B. Muñoz, W. W. Brennessel and M. L. Neidig, *Chem. Sci.*, 2018, **9**, 7931.

14 T. Parchomyk and K. Koszinowski, *Chem. – Eur. J.*, 2017, **23**, 3213.

15 T. Parchomyk and K. Koszinowski, *Chem. – Eur. J.*, 2018, **24**, 16342.

16 A Mössbauer spectrum recorded at 7 K (Fig. S2†) was essentially identical to the spectrum recorded at 80 K. No signal for iron(0) nanoparticles[17] or other low-valent iron species was observed by [57]Fe Mössbauer spectroscopy. However, unfavourable relaxation dynamics[18] may lead to pronounced line broadening that prevents detection of iron nanoparticles.

17 R. B. Bedford, M. Betham, D. W. Bruce, S. A. Davis, R. M. Frost and M. Hird, *Chem. Commun.*, 2006, 1398.

18 P. Gütlich, E. Bill and A. X. Trautwein, *Mössbauer Spectroscopy and Transition Metal Chemistry*, Springer, Heidelberg, 2011.

19 A. Casitas, J. A. Rees, R. Goddard, E. Bill, S. DeBeer and A. Fürstner, *Angew. Chem., Int. Ed.*, 2017, **56**, 10108.

20 Different fits with five subspectra are possible.

21 (*a*) S. B. Muñoz III, V. E. Fleischauer, W. W. Brennessel and M. L. Neidig, *Organometallics*, 2018, **37**, 3093; (*b*) V. E. Fleischauer, S. B. Muñoz III, P. G. N. Neate, W. W. Brennessel and M. L. Neidig, *Chem. Sci.*, 2018, **9**, 1878; (*c*) K. L. Fillman, J. A. Przyojski, M. H. Al-Afyouni, Z. J. Tonzetich and M. L. Neidig, *Chem. Sci.*, 2015, **6**, 1178; (*d*) Y. Liu, L. Wang and L. Deng, *Organometallics*, 2015, **34**, 4401.